SEPARATING BEDFORMS OF DIFFERENT SCALES IN ECHO SOUNDING DATA

Roderik C. Lindenbergh[1], Thaiënne A.G.P. van Dijk[2], Paul J.P. Egberts[2]

[1] Delft Institute of Earth Observation and Space Systems, Delft University of Technology, P.O. Box 5058, 2600 GB Delft, The Netherlands. r.c.lindenbergh@lr.tudelft.nl
[2]TNO-NITG, P.O. Box 80015, 3508 TA Utrecht, The Netherlands. thaienne.vandijk@tno.nl, paul.egberts@tno.nl

Abstract: The sea floor of the North Sea is covered by periodic bedforms of different scales. The superposition of bedforms causes difficulties for determining individual bedform parameters. In this article we compare two new methods for separating the sand wave component from the mega ripple component in Multibeam Echo Sounding measurements (MBES). One method determines a Fourier decomposition of the MBES signal, the other method uses geostatistical filtering. Both methods are described and tested on two MBES data sets of the North Sea bed. The test results correspond well. As a first application of the separation methods we determine individual bedform parameters of the separated bedforms, more particularly their wavelength and waveheight.

1. INTRODUCTION

Shallow sandy sea and river beds are often covered by harmonic bedforms of different spatial scales, changing at different temporal scales. On the North Sea floor, for example, sand waves occur with a wavelength of around 100m and a height in the order of meters covered by mega ripples that are a factor 10 smaller. The sand waves are reported to move in time scales of years, while the mega ripples move apparently much faster, more on the scale of weeks (Nemeth, 2003).
Bedforms of different scales affect the boundary layer flow conditions that cause the generation of mega ripples (e.g. Blondeaux and Vittori, 1999; Idier et al., 2004). However, it is not yet clear how sand waves and mega ripples interact dynamically. Recent observations suggest that mega ripples are moved directly by the local tidal current (Knaapen et al., 2004). Ongoing movement of the mega ripples might make the sand waves move as well. If this hypothesis is true it may be possible to predict larger scale changes of the sea floor (the sand waves) from parameters derived from smaller scale features, such as mega ripples. An example of such a parameter is the local orientation of the mega ripples (Lindenbergh, 2004; Van Dijk and Kleinhans, 2004; in press). Determination of such parameter values could therefore lead to more efficient survey planning and dredging management by those authorities that are

charting the sea floor areas and are maintaining critical navigation depths (Wüst, 2004). Understanding the dynamics of marine bedforms is also important to assess the risks for offshore constructions, such as wind farms and pipelines, and to validate scientific morphodynamic models.

Multibeam echo sounding (MBES) is the state of the art observation technique for monitoring sea floor depths (Lurton, 2002). Only MBES - in combination with the use of dGPS for horizontal accuracy - achieves the vertical accuracy and resolution, of at least one to several height observations per square meter, required for the investigation of the morphodynamics of sand waves and mega ripples. However, the superposition of bedforms complicates the analysis of individual bedform parameters, such as wavelength, wave height and wave height variations, shape and propagation direction, which are important for studying relationships between sand wave dynamics and causal factors such as flow regime. It is therefore necessary to separate bedforms of different spatial scales. Moreover, these modern digital data not only require a new data analysis approach to process the extremely large amounts of data, but an automated analysis also gives objective results, allowing to answer research questions that were not possible to answer before.

This paper aims to present and evaluate two new methods for the separation of bedforms of different scales from Multibeam data, which can be used in the morphodynamic investigation of, for example, compound sand waves. The first method is factorial Kriging, a geostatistical data analysis method (Goovaerts, 1997) and the second method is a Fourier analysis, whereby the original signal is decomposed in a series of sinusoids. Both methods are tested on MBES data on the same data of two sites in the North Sea and the results are compared and discussed.

This paper focuses on the separation of bedforms of different scales. This separation will give better insight in *(i)* the individual dynamics of sand waves, mega ripples, and larger- and smaller-scaled bedforms, *(ii)* the dynamic interaction between bedforms of different scale, and *(iii)* data artifacts. The above may answer questions such as whether sand wave dynamics are just caused by fast moving mega ripples covering the sand wave or whether sand waves actually move themselves. Apart from new evidence for the interaction between sand waves and mega ripples, the described methods will also give a more accurate description of the shape of the bedforms, which can be applied in e.g. a simulation model and can possibly be linked to local hydraulic conditions.

In section 2, we define the bedform parameters and explain the theoretical background of both the Kriging and Fourier data separation methods. In Section 3, the results of the two methods are shown on two data sets of different sand wave fields. Section 4 shows how to determine individual bedform parameters from the separated data sets. The paper ends with a discussion and conclusions and an outlook to further research.

2. METHOD OUTLINE

2.1 Parameter definitions

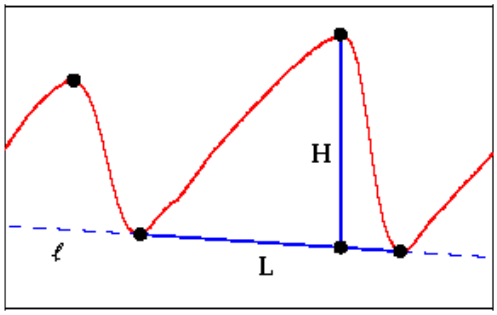

Figure 1: Sand wave height, *H*, and sand wave length, *L*.

Several definitions of sand wave parameters are used in the literature. In this paper, see Figure1, we define the *sand wave length, L,* as the distance between two adjacent trough points on the smoothed profile along the line ℓ connecting these points. The *sand wave height, H,* is the perpendicular distance from the crest point of the sand wave to the line ℓ. The term *amplitude* is reserved for the original physical definition of the distance between the mid-point and maximum extent of a wave function. The mega ripple length and height are defined analogously. The *bedform orientation* is the average angle in degrees from UTM north of the bedform crests lines, or *strike*.

2.2 Geostatistics

In this section we describe a geostatistical 2D filter method for separating an original signal into a sand wave component and a mega ripple component. A variogram analysis is used to encode the average variability of the sand wave signal. Then we show how to obtain an optimal prediction given a variogram and how to incorporate different variability in different directions. Finally we show how to filter a high frequency component within the Kriging framework.

Variogram and sand wave orientation

The presence of sand waves causes different variability in the sea floor topography in different directions. The dominant direction of the sand wave crest can be determined by a variogram analysis (Dorst, 2004). To reduce computational efforts, first a low resolution subset of a full MBES data set is selected that still represents the sand wave signal. In practice, we use a 5m grid for the variogram analysis. Let p_i denote the horizontal position of an observation, i, and z_i the depth of this observation. For some finite set of directions we determine an experimental directional variogram

$$\gamma_\alpha([h_k]) = \frac{1}{2N_k} \sum_{(z_i, z_j) \in [h_k]} (z_i - z_j)^2, \qquad N_k = \#[h_k] \tag{1}$$

Here the $[h_k]$ denotes some k-th distance class with respect to the horizontal distance between the observation positions p_i and p_j. For determining a directional variogram only those pairs (z_i, z_j) are included such that $arg(p_i\text{-}p_j) \in (\alpha\text{-}\tau\ \alpha\text{+}\tau)$, where α denotes the direction of the variogram and τ some given angular tolerance. The direction of

least variation, α_C, is parallel to the sand wave crests and the direction of maximal variation, α_P, is normal to the sand wave crests. Figure 2 shows two directional variograms, the red one parallel to the sand wave crest, and the blue one perpendicular to the crests. In this figure the dots represent the experimental variograms. The continuous lines are positive definite variogram functions fitted to the experimental variograms.

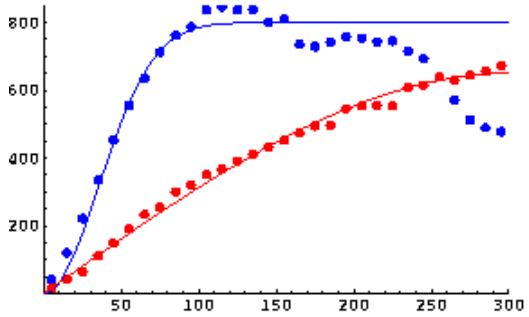

Figure 2: Directional variogram, in red parallel to the sand wave crests, in blue perpendicular to the crests. The periodicity in the blue dots represents the periodicity of sand waves. Along the horizontal axis, the distance in meter is given; the unit of the vertical axis is [dm^2].

Commonly used parameters in variogram fitting are the *range*, the distance after which the maximal variability of the signal is reached, the *sill*, the value of the maximal variability, and the *nugget*, the short range variability, that appears in the variogram as the y-axis intercept. The variability in the direction perpendicular to the crests (see Figure 2) first reaches a sill value of around 800 dm^2 at 100 m, but after that starts to decrease. This decrease is caused by the periodicity of the sand wave signal. Still, a continuous variogram is fitted to a decreasing experimental variogram, because the poor fit at larger distances does not cause any problems in the following interpolation step due to the negligible weight of observations at larger distances.

Ordinary Kriging

The Ordinary Kriging method determines the Best Linear Unbiased Predictor (BLUP) for a depth $\hat{z}_0 = \sum_{i=1}^{n} w_i z_i$ from depth observations $z_1,\ldots, z_n$, given a covariance function $cov(h) : \boldsymbol{R}^2 \rightarrow \boldsymbol{R}$, depending on the difference vector, h, between two observations. This depth prediction $\hat{z}_0$ is optimal in the sense that it minimizes the expected error variance, given the unbiasedness condition. It can be shown that this optimal solution for the weights is obtained by solving the ordinary Kriging system $C_n.w_n=d_n$, with

$$C_n = \begin{pmatrix} C_{11} & \cdots & C_{1n} & 1 \\ \vdots & \ddots & \vdots & \vdots \\ C_{n1} & \cdots & C_{nn} & 1 \\ 1 & \cdots & 1 & 0 \end{pmatrix}, \qquad d_n = \begin{pmatrix} C_{10} \\ \vdots \\ C_{n0} \\ 1 \end{pmatrix}, \qquad w_n = \begin{pmatrix} w_1 \\ \vdots \\ w_n \\ \mu \end{pmatrix}.$$

Here, C_n, denotes the *redundancy matrix* filled with covariances $C_{ij} = cov(p_i - p_j)$ between the observations. The *proximity vector*, d_n, contains the covariances $C_{i0} = cov(p_i - p_0)$ between the prediction location p_0 and the observations. Solving the system is always possible, given a positive definite covariance function, and the unique solution gives the weights $w_1,\ldots,w_n$, corresponding to the BLUP. To ensure that

the solution found is indeed unbiased, an additional condition that the weights sum up to one, is necessary. This extra condition is added to the system by means of the Lagrange multiplier μ.

Incorporating anisotropy

Assuming Second Order Stationarity, variograms and covariance functions are directly related, and the correspondence is given in the variogram by $\gamma(h) = \sigma^2 - cov(h)$, where σ^2 is the sill. From Figure 2 it is clear that the variogram value, and thus the covariance value between two positions, depends on the direction of the difference vector between the positions. Therefore we use a 2D covariance function for the Kriging system that combines the two extreme directional covariance functions, *covC*, in the direction α_C parallel to the crests, and *covP*, in the direction α_P perpendicular to the crest, compare Figure 2. For this purpose we decompose the difference vector $h = (hx, hy)$ between two positions in a crest component h_C and a perpendicular component h_P, that is, we use $\mathrm{cov}(h_x, h_y) = \frac{1}{2}(\mathrm{cov}\,C(h_C) + covP(h_P))$ with

$$\begin{pmatrix} h_C \\ h_P \end{pmatrix} = \begin{pmatrix} \cos\alpha_C & \cos\alpha_P \\ \sin\alpha_C & \sin\alpha_P \end{pmatrix}^{-1} \cdot \begin{pmatrix} h_x \\ h_y \end{pmatrix}, \tag{2}$$

to fill the redundancy matrix and the proximity factor.

Filtering

The MBES signal Z contains a sand wave component $Z_S(x, y)$ and a mega ripple component $Z_M(x, y)$. It moreover contains a noise component $Z_N(x, y)$ and maybe some other components corresponding to smaller bedforms. Therefore we can write

$$Z(x, y) = Z_S(x, y) + Z_M(x, y) + Z_N(x, y) \tag{3}$$

We want to separate the large sand wave component from the smaller components. This can be achieved by predicting $\hat{Z}_S(x, y)$ at the observation locations. For this purpose we use a slightly adapted version of Ordinary Kriging. As discussed above we can determine the variability due to sand waves by using a subset of the original data set, such that its resolution is high enough to grasp the sand wave signal, but low enough to neglect most of the smaller components. In this way we obtain the long range variograms as shown in Figure 2. Kriging with a long range means that observations on long distance still will contribute in the prediction. The sand wave component can be emphasized even more by filtering the nugget, N (Goovaerts, 1997; Wackernagel, 1998). If the nugget value N is present only in the diagonal elements of the redundancy matrix but not in the proximity vector, it will be filtered away and we will obtain $\hat{Z}_S(x, y)$ when solving the Kriging system. Moreover, the remaining signal, that is the residual $\hat{Z}_M(x, y) = Z(x, y) - \hat{Z}_S(x, y)$, gives an estimation of the mega ripple component.

2.2 Fourier analysis

A Fourier analysis is very useful for analyzing superimposed harmonic bedforms, such as compound sand waves, because it breaks down a signal into a series of constituent sinusoids of different amplitudes and frequencies. Fourier series are normally used to approximate one-dimensional harmonic time series (e.g. Priestley, 1981; Swan and Sandilands, 1994) but was also applied to aeolian bedforms (Stam,

1994). Here, we apply a Fourier analysis on MBES profiles to separate an original signal of compound bedforms into sequences of individual bedform types.

A one-dimensional sampled signal, *f*, on a length interval [0, T], can be expressed by the Fourier series:

$$f(x) = \frac{1}{N}\sum_{k=1}^{N}\left(a(k)\cos\left(\frac{F_k x}{N}\right) + b(k)\sin\left(\frac{F_k x}{N}\right)\right), \text{ with } F_k = 2\pi(k-1)\left(\frac{(N-1)}{T}\right) \qquad (4)$$

where $x \in [0,T]$ is the horizontal coordinate [m], N is the number of data points and (k-1) is the frequency. The Fourier coefficients $a(k)$ and $b(k)$ are obtained by the discrete fast Fourier transform algorithm.
A plot of the constituent sinusoids may show different groups of frequencies. For example, Figure 3(a) clearly shows three groups of frequencies, each of which - summed - would represent a bedform type. By multiple truncation of the original Fourier series (Eq. 4) at certain frequencies, (k-1), for which $1 < k < N$, that correspond to wavelengths between two bedform wavelengths, series of constituent sinusoids can be separated and grouped into different Fourier series that each represent a bedform type. These frequencies may also be determined from the power *vs.* wavelength plot (Figure 3(b)). The resulting truncated series are Fourier approximations, or smoothed curves, of the separated signals for the bedform types with the larger wavelengths. Subtraction of these approximations from the original signal results in the separated signal of the smallest bedform type.

In this paper, we use the Fourier description for the original profile (Eq. 4) and one truncated Fourier approximation for sand waves, including the larger scale topography and leaving a residual for the megaripple signal. The original input profile is a sampled signal from a Kriged grid of the real MBES data.

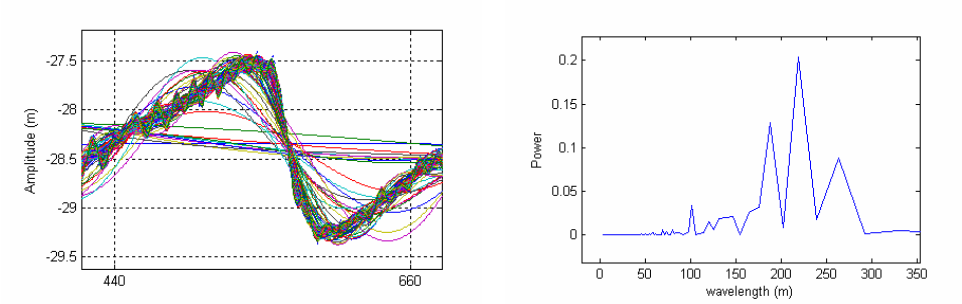

Figure 3: (a) plot of constituent sinusoids of the Fourier analysis (zoomed in), showing three groups of constituents that represent a bedform type when summed: a near horizontal large-scaled topography, sand waves and mega ripples, (b) a power *vs.* wavelength plot, indicating dominant wavelengths on sand wave scale. The mega ripple signal, at wavelengths smaller than 20 m, can only be recognized when zoomed in more. The choice of the truncation frequency corresponds to a wavelength between those bedform wavelengths.

3 DATA SEPARATION RESULTS

In this section we describe two case studies in the North Sea in which both methods of bedform separation are applied to the same data and compared. One site is the Rotterdam approach zone, 50 km offshore Rotterdam, Netherlands, and the other site is a sand wave field 50 km offshore Egmond aan Zee. Time series are available: for

Rotterdam almost yearly data exist between 1992 and 2003 and for Egmond aan Zee, 5 data sets exist between March 2001 and September 2002. However, in this paper we concentrate on the 2002 data for Rotterdam and the March 2001 set for Egmond.

3.1 MBES data sets

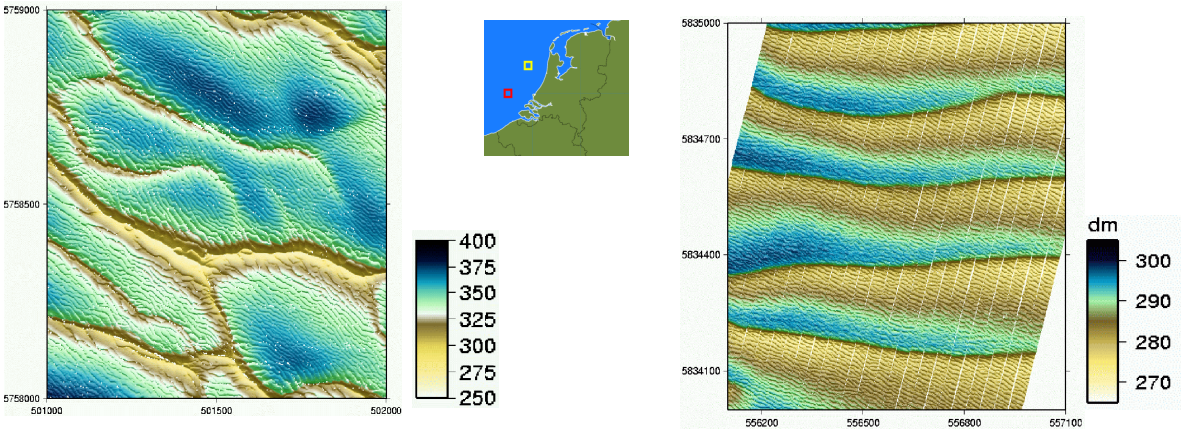

Figure 4: On the left the Rotterdam area and on the right the Egmond area. The locations of the areas are indicated on the map in the middle, where the red square corresponds to the Rotterdam area and the yellow to the Egmond area. Depths are given in decimeters.

The Rotterdam approach zone data covers an area of 1 km^2, see Figure 4. The raw MBES file of 2002 contains about 3 observations per m^2. Besides the raw data, a 5m average grid is used. This data set covers a sand wave field consisting of rather irregular sand waves of different size and height, covered by mega ripples.

On the right in Figure 4, an image of part of the Egmond data set is shown. The full data set is covering an area of 1 by 2.5 kilometers. The raw MBES data of March 2001 contains about 3 observations per m^2 as well. The sand waves in this area are much more regular, both in height and in alignment. The data set characteristics however are comparable to the Rotterdam data set.

3.2 Filtering results, Rotterdam

Filtering parameters

Firstly, the gridded data set was used for determining the input parameters for the Kriging algorithm. By comparing variograms in different directions, an average crest direction value of $\alpha_C = 67°$ was found, which implies a perpendicular direction of $\alpha_P = -23°$. For both extreme variograms, depicted in Figure 2, the sill value was set at 800 and the nugget at 10. For the crestal variogram a spherical model was used with a range of 420m and for the perpendicular variogram a Gaussian model with a range of 50m.

Secondly, the original compound signal, sampled from a 5 m averaged grid of the MBES data, was successfully described by a truncated Fourier series with frequencies up to 100. For the sand wave approximation, the series was truncated at $k = 20$ for the S-N profile along $x = 501100$ and $k = 18$ for the profile normal to the sand wave crests, which both correspond to a wavelength of 52 m. The frequency-power plot is not conclusive in this choice, but with a smaller wavelength the sand wave curve is

not smoothed sufficiently and with a larger wavelength, the sand wave signal appears in the mega ripple curve. The normal error distribution of the smoothed sand wave curve has a standard deviation of 0.3103 m for the S-N profile and 0.2946 for the profile normal to the sand wave crests, which is more than the vertical measurement error of 0.15 m.

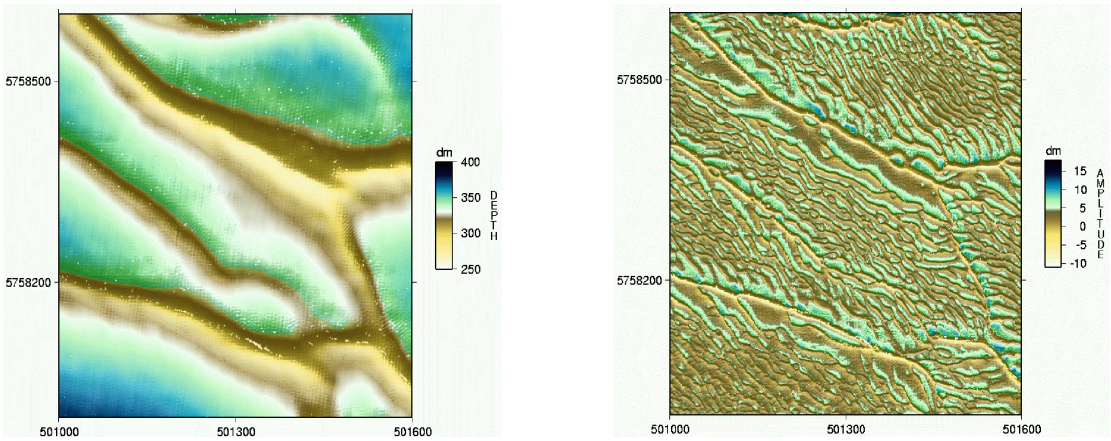

Figure 5. Two dimensional filter resulting from the geostatistical method. On the left, the sand wave signal, on the right the residual mega ripple signal. Note that most of the sand wave crests can still be recognized in the mega ripple image.

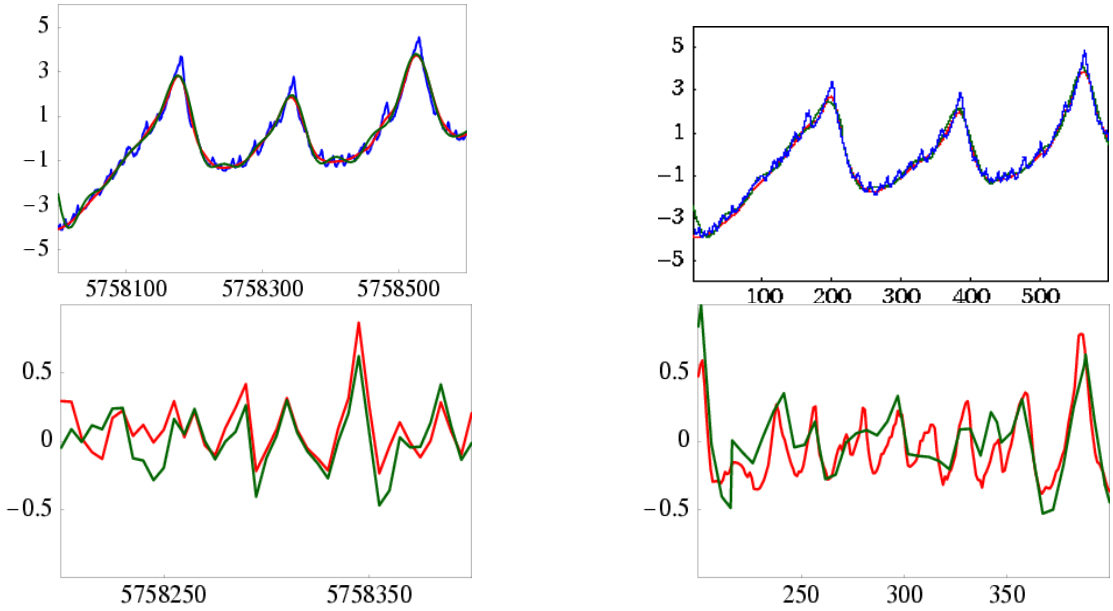

Figure 6. Filtering results of both methods. On the left the filtering results along the vertical profile x = 501100. On the right along a profile perpendicular to the crest direction, starting from (501000, 5758000) and ending at (501070, 5758600). In blue, the original signal is given, in red the results from the geostatistical method and in green the results of the Fourier method. The top pictures represent the sand waves, the bottom pictures the mega ripples. All axes are in meters.

Filtering results

In Figure 5 the 2D results of the geostatistical filtering are shown. On the left the sand wave signal is displayed, while the residual mega ripple image is shown on the right. This image gives a much clearer representation of the ripples as Figure 4. Still the

sand waves are recognizable, which could mean that near the sand waves the smoothing effect of the filter approach is too high. This could be solved by decreasing the nugget value, but tests showed that in that case parts of the ripples start to appear in the sand wave signal. A possible solution, which has not been tested yet, is to vary the value of the nugget with respect to the local sea floor depth.

The filtering results along one vertical profile and along one profile perpendicular to the crest direction are given in Figure 6. Both methods underestimate the sand wave heights. The smoothed curves of the Fourier analysis are less smooth than those from the Kriging method and still show bumps on the stoss sides of the sand waves. Although these bumps do not interfere with the determination of the bedform parameters, they do affect the mega ripple signal. In both methods, the mega ripple signal shows anomalies due to the – intentionally - poor approximation of the sand wave crests.This effect is clearly visible in Figure 6, where the largest peaks in the mega ripple signal in the two bottom figures correspond to the middle sand wave crest in the two top figures.

3.2 Filtering results, Egmond aan Zee

Filtering parameters

For the Kriging algorithm, first a 5m grid was created. A variogram analysis gave in this case a crest direction $\alpha_C = 7°$, implying a perpendicular direction of $\alpha_P = 97°$. For both extreme variograms the sill value was set at 80 and the nugget, again, at 10. For the crestal variogram a spherical model was used with a range of 500 m and for the perpendicular variogram a Gaussian model with a range of 40m.

In the Fourier analysis, the original signal, sampled from a 1 m Kriged grid of the MBES data, is described by a Fourier series with frequencies up to 1254. For the sand wave approximation, the series is truncated at $k = 52$, which corresponds to a wavelength of 52 m. The normal error distribution of this smoothed curve has a standard deviation of 0.1139 m, which is less than the measurement error.

Filtering results

In Figure 7 the filtering results along one vertical profile of the Egmond data set are shown. In this case the results of both methods are very similar. The smoothing with a truncated Fourier series is very successful. Apart from few faint bumps on the stoss slopes of the sand waves, which do not interfere with the determination of the individual sand wave parameters, the smoothed sand wave approximation is still acceptable in terms of the error standard deviation. Mega ripples are separated successfully, although - as in the Rotterdam data and the geostatistical method - an anomaly in the mega ripple signal is seen at the sand wave crests. The geostatistical method takes away again a bit too much of the sand wave crest, and the black line in the top profile shows that near the crests the differences between the two methods are maximal. The mean absolute difference between the geostatistical and the Fourier sand wave signal along the full profile of 2.5 km length is less then 8 cm with a standard deviation of 7.6cm. On top of the mega ripple signal one can even find some smaller signal.

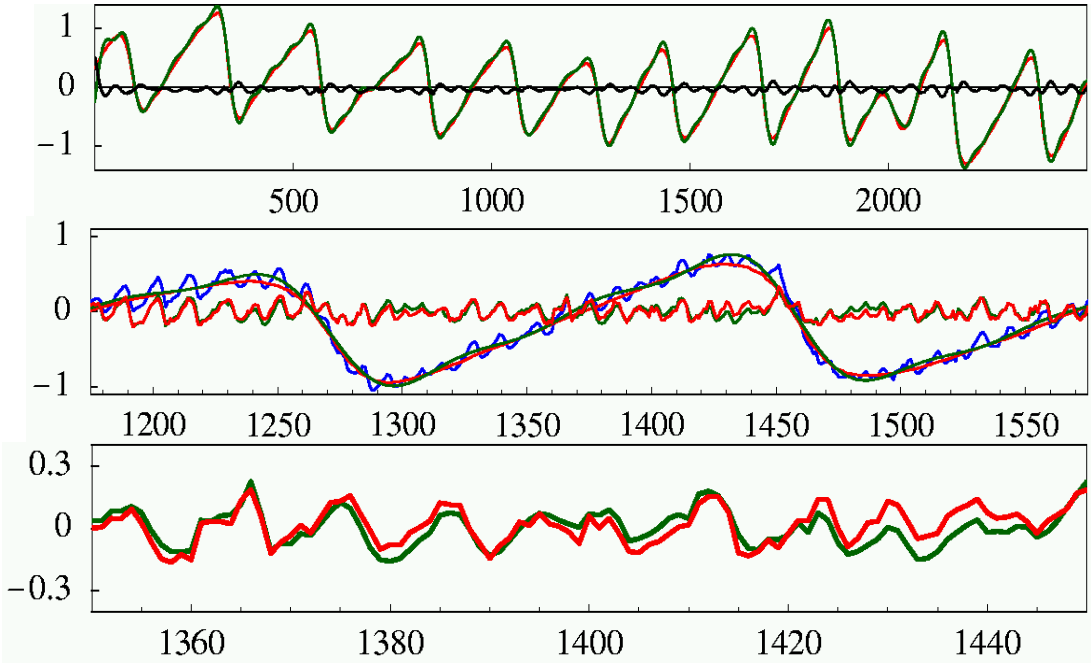

Figure 7. Filtering results of the Egmond data along a vertical profile. On top the full length profile of 2.5 km. In green the sand wave signal as found by the Fourier method, in red according to the geostatistical method. The difference between the two signals is plotted in black. The middle picture shows both the sand waves and the mega ripples along a 450m long subprofile. In blue the original signal is given as well. In the bottom picture only the mega ripples are shown along a 120m profile. All axes are in meters.

4 BEDFORM PARAMETER DETERMINATION

The main reason for developing bedform separation methods is the need for an objective automated determination of parameters describing the shape and change of the bedforms. As a first application of our separation methods, we present in this section the lengths and height of the sand waves and mega ripples along the example profiles normal to the sand wave crests that we considered.

Bedform sizes

In the Fourier analysis the *x*- and *z*-values of crest and trough points are derived from the smoothed profiles curves, by considering those points were the derivatives equal zero. In contrast to the Fourier method, the geostatistical method does not return a continuous description of the profiles, but just a discrete set of profile points. Crest and through points are found in this case by determining those profile points that are higher, resp. lower then ten nearest neighbor profile points. Once the extremes have been found, bedform wavelengths and wave heights are determined as defined in section 2.1. All bedforms sizes are derived from profiles normal to the sand wave crests with data points spaced 1 m apart, except the megaripple signal in the Fourier analysis, which the data point spacing was 5 m apart.

Sand wave height and length

The results of the sand wave height and length determination are summarized in Table 1. The Rotterdam profile of 600 m as determined by the geostatistical method contains only two complete sand waves, compare Figure 6, top right. The left sand wave has a length of 256 m, the right one of 175 m long. According to the Fourier method, the left sand wave has a length of 226 m and the right one of 184 m. The

difference between the lengths of the first sand wave is mainly due to a shift to the right of the left sand wave trough point by the Fourier method, that shows an anomaly on the left and right boundaries of profiles due to the truncation of the signal. The wave heights found by both methods vary between 2.68 and 4. 79 meter, with differences between the two methods of as little as 0.01 m to 0.73 m. Here it should be noted however that near the troughs differences between the smoothed sand wave profiles and the raw data occur of almost one meter.

The sand wave parameters along the Egmond profile, compare Figure 7, top, are based upon 11 complete sand waves in the 2.5 km profile, and are thus more reliable. In this case, the parameters, found by both methods, match very well. The average wavelength only differs 1 m between the methods. The 0.22 m difference between the average waveheights is caused by the systematic truncation of the sand wave crests by the Geostatistical method. Manual measurements in an earlier investigation (Van Dijk and Kleinhans, 2004; in press) gave a sand wave height of 1.79 m, which is very similar to the heights as found by the Fourier method.

Table 1. Sand Wave Sizes*

ROTTERDAM SAND WAVE DATA	Geostatistical method		Fourier analysis	
	wavelength [m]	waveheight [m]	wavelength [m]	waveheight [m]
Minimum	175	2.68	184	3.41
Maximum	256	4.78	226	4.79
Average	215	3.72	205	4.01

EGMOND SAND WAVE DATA	Geostatistical method		Fourier analysis	
	wavelength [m]	waveheight [m]	wavelength [m]	waveheight [m]
Minimum	131	0.64	139	0.76
Maximum	271	1.88	274	2.24
Average	208	1.55	207	1.77

* Sand wave sizes are based on 2 sand waves in the Rotterdam case and 11 sand waves in the Egmond case.

Megaripple height and length

In Table 2 the mega ripple parameters as found after filtering by both methods can be found. In the Fourier analysis of the Rotterdam profile, all points where derivatives equal zero, were used in determining the trough and crest points. This explains that even a ripple height of as small as 2 cm was found, and is also the reason that profiles with data points spaced 5 m apart give better results than a 1 m spacing. Manual editing of the input profiles, e.g. manual deselecting of some of the smaller-scaled features, may result in slightly larger values for the average ripple height and length.

In case of the profiles found by the geostatistical method, crest and trough points were obtained in the same way as for the sand waves. The average ripple length of 16.05, obtained from 37 ripples is similar to the 14.76 m as found by the Fourier method. In this case the height of the smallest ripple detected is 10 cm. The average height of 0.45 m is almost the same as the average height of 0.43 m from the Fourier method.

For the Egmond data the average ripple lengths, of 12.13 m and 12.27 m, as reported by both methods, correspond well. The average heights differ more, 0.18 m for the

Fourier case versus 0.26 m for the Geostatistical case, but this could be due to the differences in crest and trough determination methods, which do not exclude very small ripples (down to 1 cm in case of the Fourier method).

Table 2. Mega ripple sizes

ROTTERDAM MEGARIPPLE DATA	Geostatistical method		Fourier analysis	
	ripple length [m]	ripple height [m]	ripple length [m]	ripple height [m]
Minimum	5.00	0.10	7.00	0.02
Maximum	39.00	1.33	38.00	1.28
Average	16.05	0.45	14.76	0. 36

EGMOND MEGARIPPLE DATA	Geostatistical method		Fourier analysis	
	Ripple length [m]	Ripple height [m]	Ripple length [m]	Ripple height [m]
Minimum	6.00	0.11	6.00	0.01
Maximum	35.00	0.61	26.75	0.68
Average	12.13	0.26	12.27	0.18

We finish this section by concluding that even a small example shows that automatic parameter detection is possible and produces results that are comparable to results obtained manually by experts. The algorithms used for detecting single bedforms should be further evaluated however, as in the current case some anomalies are automatically accepted.

5 DISCUSSION AND CONCLUSIONS

Separation results

Both the geostatistical method and the Fourier method are successful in isolating different bedform components from 1D-profiles of digital MBES data. Results of both methods are very similar, making their effectiveness convincing. The sand wave profiles match well, except at the crests of the sand waves, where especially the geostatistical method underestimates the sand wave height. Along the mega ripple profiles, individual mega ripples of similar shape can be identified in both methods. However, due to the poor estimation of the sand wave crests, the profiles of both methods show an incorrect anomaly in the separated mega ripple signal near these crests. This anomaly in the mega ripple curve is in the same order of magnitude as the mega ripples height. This error can be avoided for both methods by using different parameters near the sand wave crests: in the geostatistical method one could decrease the nugget near the crests and one could determine the sand wave orientation locally, while in the Fourier case truncation with smaller wavelengths could solve these smoothing problems.

The automated determination of bedform parameters is an objective approach and can deal with large amounts of bedforms efficiently. However, optimizing the input parameters affects the results in both methods. This paper shows that, in the attempt to separate bedforms, optimal smoothing of the sand wave signal causes an underestimation of the sand wave heights and a good approximation of mega ripple height (e.g. the geostatistical method), and the other way around, an optimal approximation of the sand waves results in better height calculations, but underestimates the megaripple height (e.g. Fourier analysis). Choosing the parameters

still is a subjective element. Reversing the process of parameter determination could make this step more objective and efficient.

Further automatic determination of individual bedform parameters

The power of these bedform separation methods is that it allows for investigation of both morphologic parameters of individual bedforms, crucial for the explanation of cause and effect relationships in the occurrence of marine bedforms, and investigation of the interference of marine bedforms themselves, an entirely new research question. By applying more Fourier approximations in the Fourier analysis of one sequence, more scales of bedforms may be separated. In the North Sea case, for example, where wavelength ranges per bedform type do not overlap, this technique can be used to separate sand waves and mega ripples as well as long bed waves (Knaapen et al., 2001) and sand banks. These bedforms would appear as components of longer wavelengths than the sand waves in Eq. 3.
In this article we illustrate two easy methods for determining bedform heights and lengths. Other important bedform parameters can be determined automatically within the methods presented as well: the asymmetry/shape of sand waves can be defined as the ratio between the stoss and the lee sides between crest and trough points, compare Figure 1. Furthermore, an isolated two-dimensional mega ripple signal will improve the determination of local mega ripple orientations. Extending the Fourier analysis to a two-dimensional analysis will allow the determination of bedform orientations, as was achieved by the geostatistical method (Figure 5), of which results then may be compared as well.

Bedform dynamics and interaction

The research described in this paper was initiated by the wish to analyze bedform dynamics: changes in sand waves can be obscured by changing mega ripples on top of sand waves. The separation of bedforms allows the determination of morphologic changes over time of individual bedforms. Analyzing time series of morphologic and morphodynamic parameters of individual bedforms on the one hand, and causal factors, such as flow regime (hydraulic conditions) on the other hand, will bring us closer to the explanation of bed form dynamics.

ACKNOWLEDGEMENTS

Data were collected by the Directorate North Sea, Dutch Public Works and Water Management (DNZ-RWS) aboard the Ms. Arca. Simon Bicknese (DNZ-RWS) is acknowledged for providing validated digital Multibeam data and grids. Part of this work was done during the projects “Dynamics and sediment classification of the North Sea bed” (DYSC) and “Inventory of habitats of the North Sea bed” (INHABIT) of the Netherlands Institute of Applied Geosciences (TNO-NITG). This work will contribute to the MESH project (Mapping European Seabed Habitats: www.searchmesh.net) and received European Regional Development Funding through the INTERREG III B Community Initiative (www.nweurope.org).

REFERENCES

Blondeaux, P. and Vittori, G. (1999). “Boundary layer and sediment dynamics under sea waves,” in *Advances in Coastal and Ocean Engineering* 4, 133-190.

Dorst, L. L. (2004). “Survey plan improvement by detecting sea floor dynamics in archived echo sounder surveys,” *International Hydrographic Review*, 5(2):49–63.

Goovaerts, P. (1997). “Geostatistics for Natural Resources Evaluation,” Oxford University Press.

Idier, D., Astruc, D. and Hulscher, S.J.M.H. (2004). “Influence of bed roughness on dune and megaripple generation,” *Geophysical research letters*, 31, L13214, doi:10.1029/2004GL019969.

Knaapen, M. A. F., Hulscher, S.J.M.H., De Vriend, H.J. and Stolk, A. (2001). “A new type of sea bed waves,” *Geophysical Research Letters*, *28*, 1323-1326.

Knaapen, M. A. F., Van Bergen Henegouw, C.N. and Hu, Y.Y. (2004), “Quantifying bed form migration using multi-beam sonar,” report 2004R-004/WEM-007, University of Twente, Enschede, Netherlands, 16 pp.

Lindenbergh, R.(2004) “Parameter estimation and deformation analysis of sand waves and mega ripples,” In *Proceedings of International Workshop on Marine Sand Wave and River Dune Dynamics II*, Twenthe, The Netherlands.

Lurton, X. (2002) “An Introduction to Underwater Acoustics,” Springer, 2002.

Nemeth, A.A. (2003) “Modelling offshore sand waves,” published Ph.D. thesis, Universiteit Twente.

Priestley, M.B. (1981). “Spectral analysis and time series,” in: Probability and mathematical statistics, Academic Press, London, 890 pp.

Stam, J.M.T. (1994). “Process-based modeling of aeolian bedforms,” published Ph.D. thesis, Technical University Delft, Delft, Netherlands.

Swan, A.R.H. and Sandilands, M. (1995). “Introduction to geological data analysis,” Blackwell Science, Oxford, 446 pp.

Van Dijk, T.A.G.P. and Kleinhans, M.G. (2004). “Processes controlling the behaviour of sand waves and megaripples in the North Sea, The Netherlands,” In *Proceedings of International Workshop on Marine Sand Wave and River Dune Dynamics II*, Twenthe, The Netherlands.

Van Dijk, T.A.G.P. and Kleinhans, M.G. (in press). “Processes controlling the dynamics of compound sand waves in the North Sea, The Netherlands,” *Journal of Geophysical Research*.

H. Wackernagel. “Multivariate Geostatistics,” Springer, second edition, 1998.

Wüst, J. (2004) “Data-driven probabilistic predictions of bathymetry,” In *Proceedings of International Workshop on Marine Sand Wave and River Dune Dynamics II*, Twenthe, The Netherlands.